



GENERATING REALISTIC IMAGES ON THE COMPUTER THROUGH REAL LUMINOUS INTENSITY DATA AND RADIOSITY METHOD

İsmail Serkan ÜNCÜ¹, Mehmet KAYAKUŞ^{2*}

¹ Isparta Uygulamalı Bilimler Üniversitesi, Teknoloji Fakültesi, Elektrik-Elektronik Mühendisliği Bölümü, Isparta, Türkiye

² Akdeniz Üniversitesi, Manavgat Sosyal ve Beşerî Bilimler Fakültesi, İşletme Enformatiği Bölümü, Antalya, Türkiye

Keywords

*Radiosity 1,
Luminous intensity 2,
Realistic images 3,
Image processing 4,*

Abstract

Simulation of luminous distribution and modeling techniques are widely used in generating realistic images. It is performed by modeling the interaction of light with an individual surface and combining emission, transmission and reflection effects among all the surfaces in the environment. In this study, a realistic image was generated in the simulation area created in computer environment by using real luminous intensity data. It was aimed to generate a realistic image of a table and chair in the simulation environment. A goniophotometer was used to obtain the real luminous intensity curves of the luminaire to be used in the simulation environment. Realistic images were generated by using the real luminous intensity data obtained by the goniophotometer through the radiosity method. Radiosity method was used to transfer the luminous intensity data to the computer. The level for stopping the radiosity method was decided through histogram analyses that were performed by using image processing techniques. When the change in the mean brightness value in the histogram value was 1% and below, iteration was stopped by the software. According to the results of the tests performed on the given example, it was observed that the real image could be generated after approximately 3000 iterations and that the change decreased below 1% after this value.

BİLGİSAYAR ORTAMINDA GERÇEK IŞIK ŞİDDET VERİLERİ VE RADİOSİTY YÖNTEMİ KULLANILARAK GERÇEKÇİ GÖRÜNTÜLERİN OLUŞTURULMASI

Anahtar Kelimeler

*Radiosity 1,
Işık şiddeti 2,
Gerçekçi görüntüler 3,
Görüntü işleme 4,*

Öz

Gerçekçi görüntü oluşturmada ışığın yayılmasını simüle etme ve modelleme teknikleri oldukça yaygın kullanılan tekniklerdir. Işığın bireysel bir yüzeye etkileşiminin modellenmesi ortamdaki tüm yüzeyler arasında emisyon, iletim ve yansıma etkilerinin birleştirilmesiyle gerçekleşmektedir. Bu çalışmada gerçek ışık şiddet verileri kullanılarak; bilgisayar ortamında oluşturulan simülasyon alanında gerçekçi bir görüntü oluşturulmuştur. Simülasyon ortamında bir masa ve sandalyeden oluşan gerçekçi bir görüntünün oluşması amaçlanmıştır. Simülasyon ortamında kullanılacak armatürün gerçek ışık şiddet eğrilerini elde etmek için goniofotometre kullanılmıştır. Goiofotometre ile elde edilen gerçek ışık şiddet verileri radiosity metodunda kullanılarak gerçekçi resimler elde edilmiştir. Işık şiddet verilerinin bilgisayar ortamına aktarımında radiosity metodu kullanılmıştır. Radiosity yönteminin hangi seviyede durdurulacağına görüntü işleme teknikleri kullanılarak elde edilen histogram analizleri ile karar verilmiştir. Histogram değerinde ortalama parlaklık değerindeki değişim %1 ve altında bir değere ulaştığında yazılım iterasyonu durdurulmuştur. Verilen örnek için yapılan testler sonucu yaklaşık 3000 iterasyondan sonra gerçek görüntünün oluşması sağlandığı; bu değerden sonra değişimin %1'in altına indiği görülmüştür.

* İlgili yazar / Corresponding author: mehmetkayakus@akdeniz.edu.tr +90-242-742-7025

Alıntı / Cite

Üncü, İ.S., Kayakuş, M., (2020). Generating Realistic Images On The Computer Through Real Luminous Intensity Data And Radiosity Method, *Mühendislik Bilimleri ve Tasarım Dergisi*, 8(5), 255-270.

Yazar Kimliği / Author ID (ORCID Number)

Yazar1 İ.S. Üncü, 0000-0003-4345-761X
Yazar2 M. Kayakuş, 0000-0003-0394-5862

Makale Süreci / Article Process

Başvuru Tarihi / Submission Date	15.11.2020
Revizyon Tarihi / Revision Date	16.12.2020
Kabul Tarihi / Accepted Date	16.12.2020
Yayın Tarihi / Published Date	29.12.2020

1. Introduction

One purpose of computer graphics is to produce realistic pictures quickly and accurately. For this purpose, local, intuitive shading models have been replaced by increasingly complex techniques such as ray tracing and radiosity (Drucker & Schröder, 1992; Goral, Torrance, Greenberg, & Battaile, 1984; Whitted, 1979).

Generation of realistic images requires the ability to simulate the luminous distribution in an environment. This requires two steps: Modelling the interaction of light with an individual surface and combining emission, transmission and reflection effects between all surfaces in the environment. In the past, computer-generated images were obtained by simulating the way light was reflected from a single surface, neglecting surface-to-surface interactions. There are a number of reflection models ranging from a simple model, in which all light is reflected equally in all directions, to more complex models that include uneven distributions based on geometric and electromagnetic properties of the surface. For any reflection model, images are generated by determining the visible surface for each screen pixel and then calculating the intensity of the light leaving that surface in the eye direction. This intensity typically consists of geometrical relationships between visible surface, light sources and the eye (Immel vd., 1986).

Generating realistic images requires the assessment of a shading model that simulates the luminous distribution in an environment. Shading models, where shading is calculated based solely on direct illumination of light sources, are frequently used to obtain the images quickly. However, realistic shading requires the use of a lighting model, which considers the secondary lighting provided by light reflected from other surfaces and the shading of one surface by another (Wallace vd., 1989). Visible light needs to be modelled correctly for generating realistic computer images. Radiosity method has proven to be a useful approach for computer graphic lighting calculations (Baum vd., 1989).

Generation of realistic images requires the calculation of luminous intensity, leaving visible surfaces on each pixel of the image plane in the direction of the observer. Methods for calculating this intensity are based solely on the principle of direct illumination of surfaces by light sources. More sophisticated methods started to be used for global lighting, which included the impact of all objects in the environment. In the radiosity approach, all calculations are independent of view. The standard radiosity method only results in scattered surfaces. The set of sample points, where the intensities are calculated, depends on the separation of the media surfaces instead of the viewpoint and image resolution (Wallace vd., 1987).

Radiosity method started to be developed in 1950s to calculate radiosity transfer between surfaces (Howell vd., 2010). Borrowed from thermal engineering techniques, the radiosity method was introduced by Goral in 1984 in the context of computer graphics (Sparrow, 2018; Goral vd., 1984). In 1984, the first solutions of luminous activity generated by Nishita and Nakamae began to be applied in image synthesis (Nishita and Nakamae, 1985). In general, radiosity methods are used to solve the internal reflection of light between scattered surfaces. The first algorithms were limited to environments where all surfaces could face each other. In the following years, radiosity algorithms developed and the sensitivity increased as the environment was divided into pieces independently.

Radiosity algorithm is a method used for evaluating the intensity or radiosity in discrete points and surface areas in an environment (Cohen vd., 1987). The radiosity method is often referred to as a view independent technique. In simulations, this method is used to view the environment from different angles. The original luminous activity method was based on the diffuse reflection assumption of Lambert; however, subsequent studies also included radiosity approaches along with full reflection. In 1988, Cohen introduced the "advanced sensitization" approach, which allowed faster solutions for generating images in the computer environment (Cohen vd., 1987). In 1991, Hanrahan created the formula that be-longed to the entire hierarchical radiosity system (Hanrahan vd., 1991). All these developments emerged as a serious step in defining and decomposing surfaces.

The most important advantage of the radiosity method is that the solution is independent of view. Pre-calculated densities of light could be used for the interactively oriented synthetic environment in the radiosity method (Baum vd., 1989; Zhu vd., 1989).

In realistic generation, the radiosity method requires strong computational power and high memory costs. As a solution, Form factors can be calculated in parallel and independently in several processors; thus, a high acceleration can be achieved in this most computational task. These parallelizations of the radiosity approach lead to an extraordinary acceleration in image creation (Drucker & Schröder, 1992; Purgathofer & Zeiller, 1992).

There is intensive work on realistic images using the radiosity method. In one of these, it added multiplication texture effects to the radiosity method. Thanks to a texture effects included in the radiosity solution process, improvements have been achieved for perturbed surfaces(Chen & Wu, 1990).

In this study, a realistic image was generated in the simulation area created in computer environment by using real luminous intensity data. It was aimed to generate a realistic image of a table and chair in the simulation environment. A goniophotometer was used to obtain the real luminous intensity curves of the luminaire to be used in the simulation environment. Realistic images were generated by using the real luminous intensity data obtained by the goniophotometer through the radiosity method. Radiosity method was used to transfer the luminous intensity data to the computer. The level for stopping the radiosity method was decided through histogram analyses that were performed by using image processing techniques. When the change in the mean brightness value in the histogram value was 1% and below, iteration was stopped by the software. According to the results of the tests performed on the given example, it was observed that the real image could be generated after approximately 3000 iterations and that the change decreased below 1% after this value.

2. Material and Method

A goniophotometer, which could derive the real luminous intensity curve data of the luminaire to be used in the simulation environment on the C plane, was used. These data were transferred to the simulation environment with the radiosity method to create the conditions for real image.

2.1. Goniofotometre

Goniophotometer is the name of the system, which is established to examine the luminous intensity distribution in a light source through one fixed light source or photometric head and another with regular movements (Sirel, 1997). In the system, which operates by moving the luminaire, a type 3 goniophotometer was selected according to the C plane due to its high speed in examining the angular variation of the photometric size and the little amount of space it occupied. Figure 1 presents a goniophotometer, which could derive the real luminous intensity data of a luminaire on the C plain.



Figure 1. Goniophotometer

Luminous intensity data is obtained with the help of a lux meter placed against the goniophotometer by using the lighting luminaire connected to the goniophotometer mentioned above.

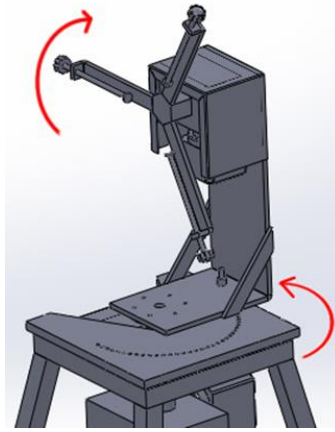


Figure 2. Working structure of the system

To enable the luminaire to make these movements through software, computer-operated step motors are used. As presented in Figure 2, the first step motor rotates luminaire around its axis while the second step motor rotates the motor from right to left.

In accordance with the information entered, the software calculates the luminous intensity with the Equation (1) according to each step. In this formula, E indicates the illuminance level (lux) measured by the lux meter, r indicates the measurement distance (meters), and ϵ_2 indicates the angle of incidence.

$$I = Er^2 \cos \epsilon_2 \pi_0 \quad (1)$$

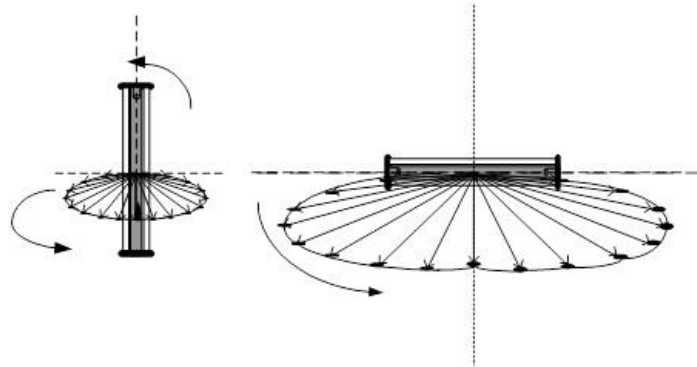


Figure 3. Luminaire intensity curves

The luminous intensity data generated according to the luminaire position using the linear luminaire intensity curves given in Figure 3 are presented in the table in Figure 4.

Veri Modelleyici - 2003.06.17 11:37											
Yolay Veri	11	Dikay Veri	19	Işık-Siddet Eğrisi		Veri -> Denetim					
	0	2	3	4	5	6	7	8	9	10	11
1	470	946	1749	2128	2317	2609	3003	3602	4075	4571	4892
2	766	1303	1754	1776	2342	2769	2959	3396	4148	4369	4656
3	940	850	1608	2091	2594	2701	3291	3573	3840	4667	5125
4	458	970	1319	1969	2444	2743	3438	3388	3855	4568	4787
5	421	948	1437	1874	2432	2960	3421	3407	4149	4665	4951
6	471	1021	1700	1824	2579	2559	3267	3383	4174	4450	4835
7	744	1298	1723	1992	2522	2866	3254	3447	3901	4427	5051
8	525	1211	1345	2063	2400	2754	3391	3640	4085	4532	4870
9	600	1158	1760	2140	2568	2682	3185	3829	4103	4554	4950
10	869	1264	1548	1697	2261	2970	3353	3690	3898	4529	4989
11	430	1211	1661	1690	2581	2904	3345	3458	4232	4379	4937
12	706	1258	1530	1725	2207	2905	3201	3759	3934	4422	5030
13	503	1114	1280	1787	2260	2877	3377	3442	4227	4567	4929
14	841	1219	1371	2067	2501	2551	3050	3573	3906	4347	5095
15	706	1271	1477	2052	2139	2863	3384	3617	4146	4471	4851
16	699	1161	1684	2001	2534	2577	3099	3591	4106	4698	4893
17	583	1273	1669	2128	2276	2947	2970	3623	4251	4379	4717
18	652	955	1729	1792	2211	2947	3378	3813	4089	4423	4953
19	763	967	1380	1979	2422	2590	3171	3500	3890	4694	4865

Figure 4. Presentation of luminous intensity data according to the position of the luminaire

The least squares method was used to draw curves among the luminous intensity data. In the least squares method, let's assume that given points are (i, y_i) and the points of the approach are (i, Y_i) . In this case, the condition would be,

$$\sum_{i=1}^n (Y_i - y_i) = \text{minimum} \quad (2)$$

If $n=2$, then

$$\sum_{i=1}^2 (Y_i - y_i) = \text{minimum} \quad (3)$$

However, as presented in Figure 5, there is no affinity between $y=p(x)$ interpolation line and $y=f(x)$ main line.

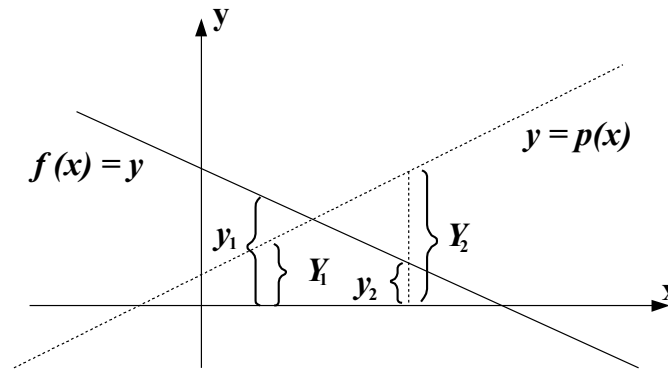


Figure 5. Demonstration of interpolation curves

Therefore, instead of Equation (3),

$$\sum_{i=1}^2 |(Y_i - y_i)| = \text{minimum} \quad (4)$$

should be considered (Baum vd., 1989). However, since absolute functions do not have derivatives at the point where they pass the minimum, derivatives cannot be taken to find the minimum. For this reason, the following equivalent of Equation (3), which enables derivation, is considered:

$$S = \sum_{i=1}^n (Y_i - y_i)^2 = \text{minimum} \quad (5)$$

Thus, an expression, which has a minimum and whose partial derivative could be calculated, is obtained. The polynomial equation passing through the given points are found using the least squares method.

Where (i, y_i) , $i=1(1)n$ are the given points, a polynomial curve passing through these points and of $m(m \leq n)$ degree could be found by least squares method as follows:

$$Y = C_0 + C_1x + C_2x^2 + \dots + C_nx^n \quad (6)$$

The luminous intensity curves of the luminous intensity data according to the position of the luminaire are expressed as in Equation (5). If the partial derivative of the equations that minimize each point equation is taken and equalized to zero to determine the C coefficients in the equation, it will be as follows:

$$S = S(C_0, C_1, \dots, C_m) = \sum_{i=1}^n (Y_i - y_i)^2 \quad (7)$$

$$\left(\sum_{i=1}^n x_i^m \right) C_0 + \left(\sum_{i=1}^n x_i^{m+1} \right) C_1 + \dots + \left(\sum_{i=1}^n x_i^{m+n} \right) C_m = \sum_{i=1}^n x_i^m y_i \quad (8)$$

This system consists of $(m+1)$ equations and $(m+1)$ unknown. Obtained C_0, C_1, \dots, C_m values are determined. Luminous intensity curves form three-dimensional luminous intensity distributions. Luminous intensity curve could be drawn by finding the C coefficients of these equations. The luminous distribution curves of the luminaire to be used in the study are presented in Figure 6.

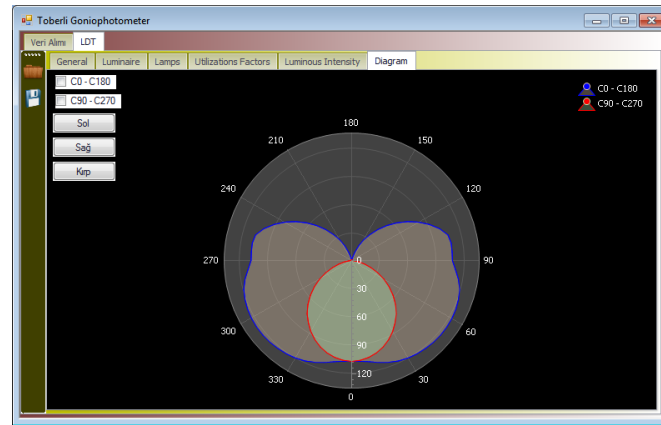


Figure 6. Luminous intensity curve of the luminaire

2.2. Radiosity method

Radiosity method was used in order to ensure that the luminaire could generate a realistic image in the simulation area created in computer environment. Realistic images were obtained using the real luminous intensity data obtained with the goniophotometer in the starting radiosity formula.

In terms of the classic radiosity equation, all surfaces of a scene (light sources are also modelled as surfaces) are viewed as Lambert reflectors and split into small surface elements called patches. It is important that the patches are homogeneous in light distribution and reflection properties. A form value is calculated using the formula for each patch; a minimum of three values (RGB) are required in computer graphics. This form value corresponds to the light distributed by the patch, which is the sum of the light it reflects and emits. The reflected light depends on the incoming light reflected by other patches and the reflection factor of the patch, which indicates the amount of energy absorbed by the area per wavelength.

2.3. Luminous intensity for the light source, which could be represented by the luminous intensity curve

The distribution of energy from the light source that could be represented by a luminous intensity curve is outward from the center. The amount of beam is expressed according to its angle with the area where the given intensity is reflected in a given direction.

$$d\Phi = I(\varpi)d\varpi \quad (9)$$

In the Equation (9), $d\Phi$ indicates the luminous flux, $I(\varpi)$ indicates the luminous intensity of the light source that could be represented by a luminous curve, and $d\varpi$ indicates the small light beam. Luminous intensity for the light source, which could be represented by the luminous intensity curve is expressed as follows:

$$I = \frac{\Phi}{4\Omega} \quad (10)$$

Thus, the total light flux ingested Φ becomes the following:

$$\Phi = \int I(\varpi)d\varpi \quad (11)$$

The brightness level E occurring in a differential area from the light source that could be represented by a single luminous intensity curve could be calculated by finding the angle surrounded by the surface element when viewed from the light source.

$$E = I \frac{d\varpi}{dA} = \frac{\Phi}{4\Omega} \frac{\cos \theta}{|x - x_s|^2} \quad (12)$$

$|x-x_s|$ indicates the distance from the point to the surface element.

2.4. Rendering equation

Reflection equation makes it possible to calculate the reflected luminous distribution based on the distribution of incoming light and BRDF (bidirectional reflection distribution function) of the material. The first and most preferred model is direct lighting resulting from simple light sources. The environment is not considered as a

whole and the surfaces shaded by the properties of the light sources are taken into account. This lighting model is called local lighting. Shadows could be added by testing whether a spot on the surface is visible to the light source. This model, which takes into consideration the entire environment, is an example of global (general) lighting. The second and truly difficult situation is indirect lighting. In this case, the light can come from any surface in the environment and shading is very important (Sillion and Peuch,1994).

2.5. Local or direct lighting

Reflection equation is expressed as follows:

$$R_r(\omega_r) = \int_{\pi_i} f_r(\omega_i \rightarrow \omega_r) R_r(\omega_i) \cos \theta_i dw_i \quad (13)$$

Similarly, the level of light obtained from the light source that could be represented by a luminous intensity curve is expressed as follows:

$$E = \frac{\Phi \cos \theta}{4\pi |x - x_s|^2} \quad (14)$$

If the direction of the light source is expressed with ω_s , then the dose of a light source that could be represented by a luminous intensity curve, is expressed by a delta function as follows: $L_i(\omega_i)$;

$$R_i(\omega_i) = \frac{\Phi}{4\pi |x - x_s|^2} \delta(\cos \theta_i - \cos \theta_s) \delta(\varphi_i - \varphi_s) \quad (15)$$

If the above equation is substituted in the reflection equation;

$$R_r(\omega_r) = \frac{\Phi}{4\pi |x - x_s|^2} f_r(\omega_r - \omega_s) \cos \theta_s \quad (16)$$

2.6. Global or indirect lighting

In the first step, the lighting on one surface is associated with the distribution of light coming from another surface. Based on the fact that the dose is constant across a surface, the dose that falls on x' , which consists of the dose on x , is calculated.

$$R_i(x' \frac{r}{\omega_i'}) = R_o(x, \frac{r}{\omega_o}) V(x, x') \quad (17)$$

Here, ω_i indicates the direction vector from x' to x . Where ω_o it is the direction vector from x to x' .

$$\omega_i = -\omega_o = \frac{x - x'}{|x - x'|} \quad (18)$$

$V(x, x')$ is the visibility function. If x and x' are absolutely visible, their value would be 1; otherwise it would be zero. The next step is to convert the semispherical integral obtained from all incoming directions into the field integral that are obtained from all fields in the environment. The angle projection converted by the source could easily be transformed by associating it with the passive surface areas formed.

$$dw_i' = \frac{\cos \theta_o dA}{|x - x'|} \quad (19)$$

If this equation is multiplied by the angle of projection; then,

$$dw_i' \cos \theta_o dA = G(x, x') dA \quad (20)$$

The value of the $G(x, x')$ geometric function is as follows:

$$G(x, x') = G(x', x) = \frac{\cos \theta'_i \cos \theta_o}{|x - x'|^2} \quad (21)$$

If the $G(x, x')$ value is placed on the reflection equation, the equation turns into an integral equation over the S surfaces.

$$R(x', \varpi') = \int_s f_r(x) R(x, \varpi) G(x, x') V(x, x') dA \quad (22)$$

Since doses coming from this equation also includes the direction, the elements representing the arrival and exit directions could be found. The equation given above was first introduced to graphics software on the computer by Kajiya under the name of rendering equation. This intensity of two point transfer from x' to x is expressed by the $I(x, x')$ symbol. The density measure is only a function related to the surface position and does not include circumferential angles. The light flux between two points is expressed in Equation (23).

$$d\Phi = I(x \rightarrow x') dA dA' = R(x, \varpi) G(x, x') dA dA' \quad (23)$$

Figure 7 presents the transfer geometry of two points.

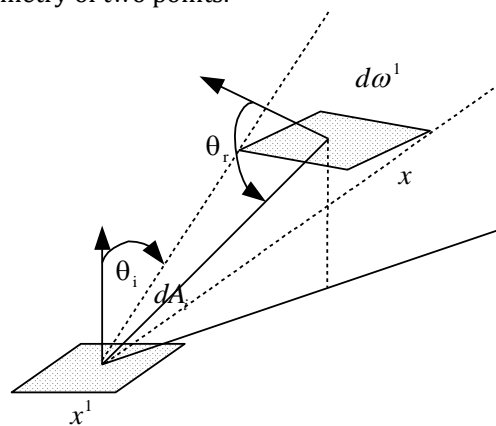


Figure 7. The transfer geometry of two points

It is the flux of light flowing in the beam that connects dA' to dA . If two sides of the equation are multiplied by $G(x', x'')$ $dA' dA''$, it could be turned into the following form: The Equation after the multiplication is as follows:

$$I(x \rightarrow x'') = G(x', x'') \int_s f_r(x \rightarrow x' \rightarrow x'') V(x, x') I(x \rightarrow x') dA \quad (24)$$

2.7. Radiosity equation

All surfaces in the radiosity environment are assumed to be homogeneous diffuse reflectors in accordance with the Lambert principle. Thus, BRDF is independent of incoming and outgoing directions and could be removed from the integral.

$$R(x' \rightarrow x'') = R_e(x' \rightarrow x'') + f_r(x') \int_s R(x \rightarrow x') G(x, x') V(x \rightarrow x') dA \quad (25)$$

$$R(x' \rightarrow x'') = R_e(x' \rightarrow x'') + \frac{\rho(x')}{\pi} \int_s R(x \rightarrow x') G(x, x') V(x \rightarrow x') dA \quad (26)$$

In homogenous reflection, the radiation emanating from a surface is the same in all directions and is equal to the radiosity B divided by π . This leads us to some simplifications. Rendering equation expresses the position of light energy at all points in space (Cohen and Wallace, 2012).

$$B(x) = E(x) + p(x) \int_s B(x') \frac{G(x, x') V(x \rightarrow x')}{\pi} dA' \quad (27)$$

Hence, the radiosity equation could be found.

2.8. Form factor

In the radiation method, determining the form factors bears most of the calculations. In an N-surface environment, N^2 form factors should be determined (Baum vd., 1989). Equation (28) shows the formula of form factor differential equation. The element-to-element form factor is a double-field integral, including the geometric basis of G_{ij} .

$$F_{ij} = \frac{1}{A_i} \int_{A_i} \int_{A_j} \frac{\cos \theta_i \cos \theta_j}{\pi r^2} V_{ij} dA_j dA_i \quad (28)$$

Figure 8 presents the form factors of the two base functions. In the equality, the term V_{ij} is the visibility term between the differential areas of dA_j and dA_i .

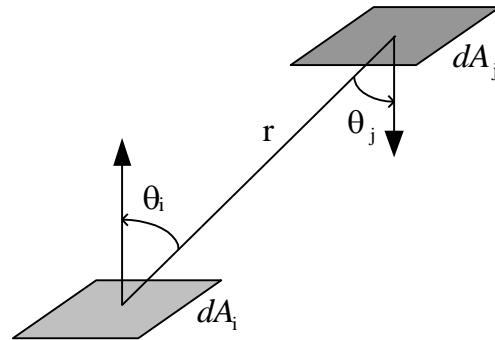


Figure 8. The form factors of the two base functions

2.9. Radiosity of fixed elements

In the equations given above, if the reflection and absorption that is assumed to be fixed in all elements and the fixed base functions are used, then the complexity is reduced. Galerkin formula could be written for the fixed base functions of N_i . First of all, the box base functions known to take only the values of 1 and 0 are used.

$$\int_s N_i(x) N_j(x) dA = \begin{cases} A_i, & i = j \text{ ise} \\ 0, & \text{aksi halde} \end{cases} = \delta_{ij} A_i \quad (29)$$

Here, δ_{ij} defines the Kronecker delta, and A_i defines the area of the element no i. Likewise, the absorption function is defined as follows:

$$\int_s E(x) N_i(x) dA = E_i A_i \quad (30)$$

The term E_i refers to the average absorption value of the area that belongs to the element i (Wolfe, 2000). Base functions can be extracted from the integral where they have unit values. Moreover, it is assumed that the reflection function of $\rho(x)$ receives a fixed pi value on A_i .

$$\int_s N_i(x) \rho(x) \int_s N_j(x') G(x, x') dA' dA \quad (31)$$

$$\rho_i \int_{A_i} \int_{A_j} G(x, x') dA_j dA_i \quad (32)$$

If the equation is evaluated for each i, the results will be as follows:

$$\left[\sum_{j=1}^n B_j \left[\delta_{ij} A_i - \rho_i \int_{A_i} \int_{A_j} G(x, x') dA_j dA_i \right] \right] = -E_i A_i = 0 \quad (33)$$

If it is divided by a_i and the absorption term is taken to the right of the equation, the following equation is obtained:

$$\left[\sum_{j=1}^n B_j \left[\delta_{ij} A_i - \rho_i \frac{1}{A_i} \int_{A_i} \int_{A_j} G(x, x') dA_j dA_i \right] \right] = -E_i \quad (34)$$

or

$$\left[\sum_{j=1}^n B_j [\delta_{ij} - \rho_i F_{ij}] \right] = -E_i \quad (35)$$

The F_{ij} specified in the previous formula is called the form factor and is expressed as follows: Form factor, indicates the energy that leaves the element i divided by the energy reaching element j . As with previous formulations, linear system equations can be expressed by matrix equation, $KB = E$. K input values are found as follows.

$$K_{ij} = \delta_{ij} - \rho_i F_{ij} \quad (37)$$

Here, if Equation (27) is re-evaluated, classical radiosity equation is obtained.

$$B_i = E_i + \rho_i \sum_{j=1}^n B_j F_{ij} \quad (38)$$

If it is multiplied by A_i ,

$$B_i A_i = E_i A_i + \rho_i \sum_{j=1}^n B_j F_{ij} A_i \quad (39)$$

and if the rule of equality between form factors is used, then:

$$F_{ij} A_j = F_{ji} A_i \quad (40)$$

$$B_i A_i = E_i A_i + \rho_i \sum_{j=1}^n B_j F_{ij} A_i \quad (41)$$

The physical interpretation of this equation is that the total power that leaves an element, $B_i A_i$, depends only on the beams that the element directly absorbs and reflects. This reflected light depends on the dose that separates from all the elements in the environment. A part of the dose that separates from the elements in the environment could again come back to an element. This dose varies depending on the geometric relationship between the elements and the reflection of the elements (Cohen vd., 1986).

3. Application of radiosity method

The basic steps required to formulate the general radiosity method and to solve it with software are as follows:

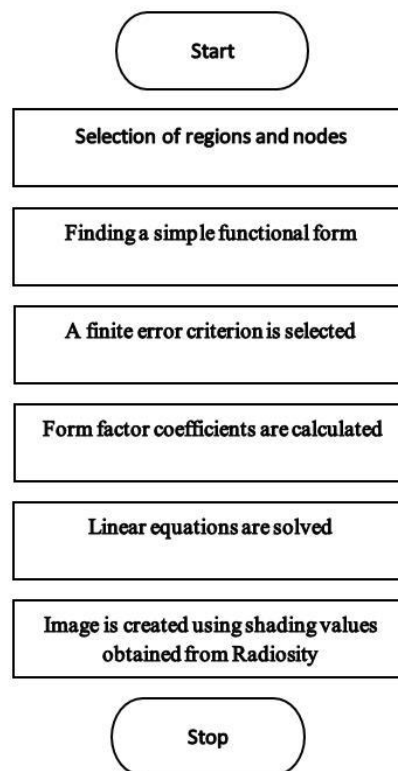


Figure 9. The luminous activity method calculation algorithm

In the luminous activity method calculation algorithm presented in Figure 9, first, the areas are divided into sub elements as can be seen in the steps in the flow chart. Regions or nodes where exact radiosity values would be calculated are selected on the elements. There is a simple functional form for variable radiosity values on an element. A finite error criterion is selected. This brings the error closer to a finite sum. Thus, the infinite problem turns into a finite number of linear equations. Coefficients of the linear system are calculated. These coefficients, which are called form factors, depend on the geometric relations that allow light to pass between the elements. Linear equations are resolved for unknown point radiosity values. The approximate radiosity result is reconstructed as a linear sum of the base functions created predominantly with point radiosity values. The image is generated using the shading values obtained from the radiosity approach for the desired view direction.

In general, radiosity methods are used to solve the internal reflection of light between scattered surfaces. The first algorithms were limited to environments where all surfaces could face each other. Therefore, it is used in indoor areas. Radiosity algorithms have evolved over time and the sensitivity of the medium has been increased by separating the pieces independently (Baum vd., 1989). When switched to the radiosity area from the control screen, the sample area is loaded directly into the system.

When the data of an armature is loaded into a three-dimensional virtual space with the Radiosity method, the starting position is given in Figure 10.

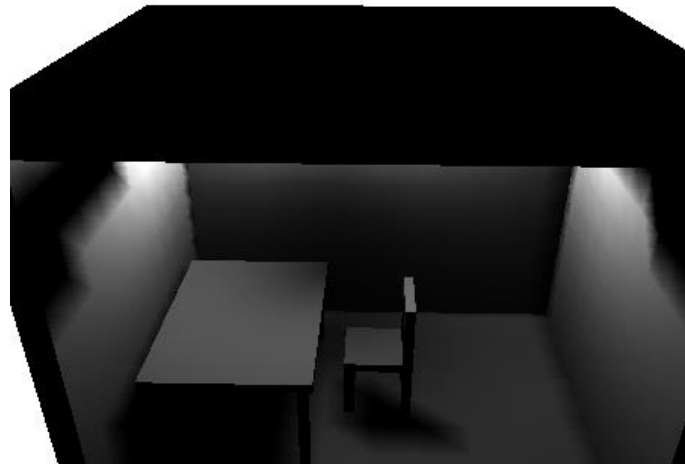
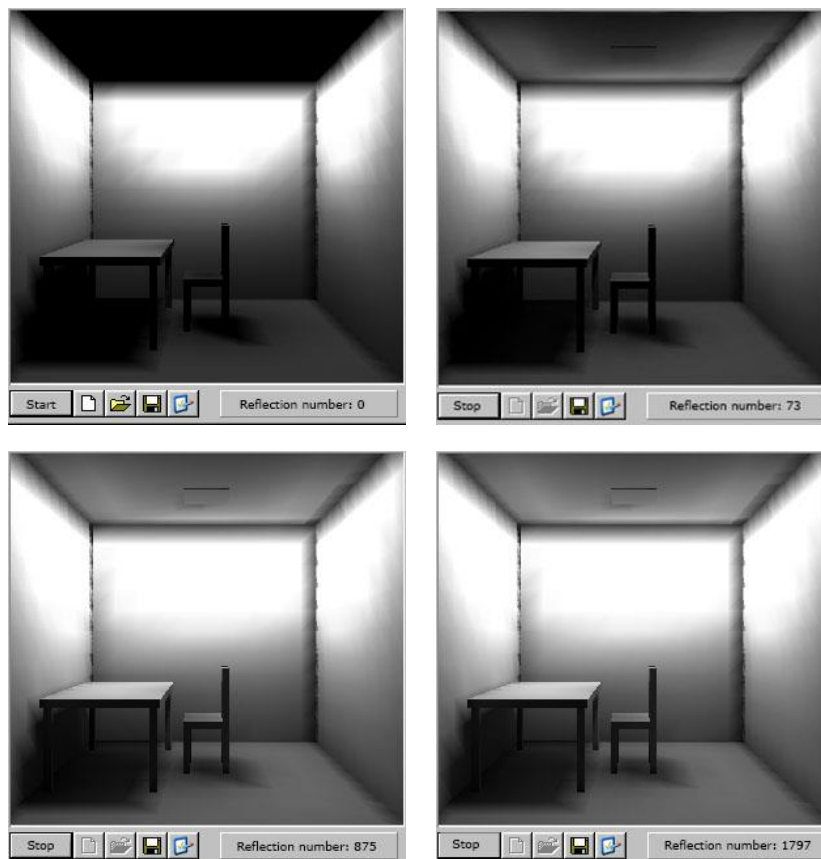


Figure 10. The starting position radiosity method

By examining from different points of view on the images that are generated realistically, the user can make various aesthetic and technical evaluations such as the location of the light sources, color of the wall, positions of the furniture and the whether the items would remain in the shade according to the light in the computer environment. According to the different numbers of reflection displayed in Figure 11, it is observed that the image quality increases as the number of reflections increases in the radiosity tests performed. However, infinite number of reflections causes the generated image to be viewed brighter than it is. Therefore, a limit should be placed on the number of reflections.



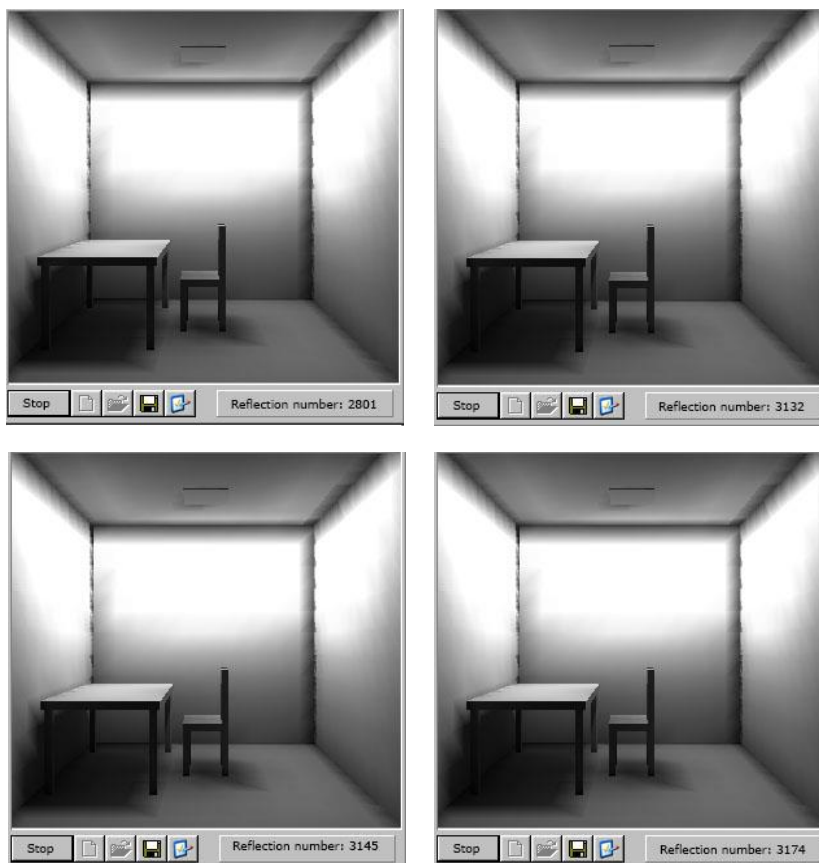


Figure 11. Radiosity according to different reflection numbers

4. Results and Discussion

As a result of the studies, when the change was fixed with the histogram technique according to the reference shading area, the reflections were stopped by the software. This stopping rule is determined as the brightness falling below 1% in the histogram. Figure 12 presents the histogram change according to the number of reflections.

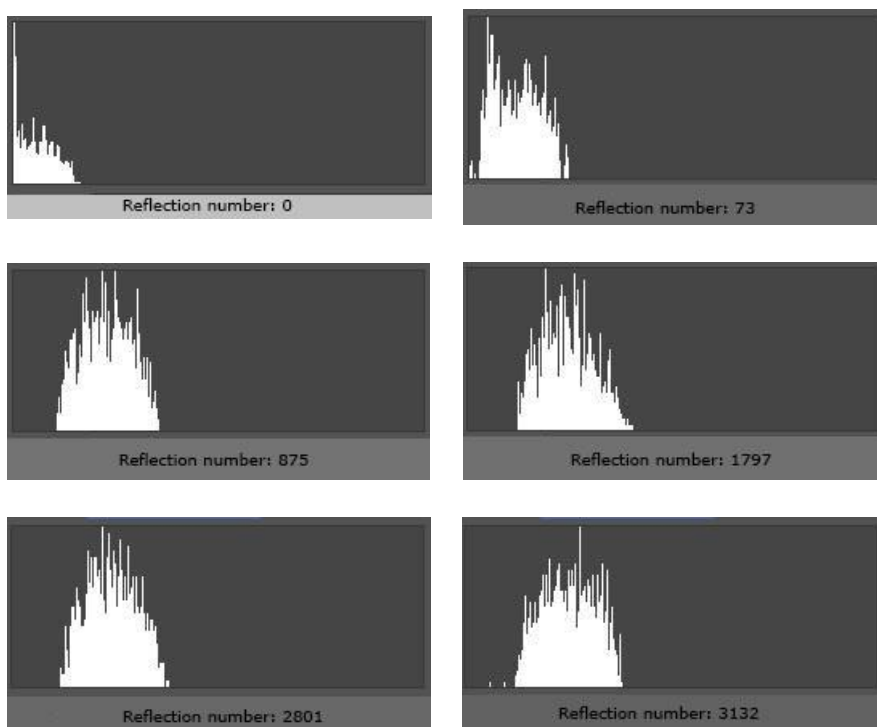




Figure 12. Histogram change according to the number of reflections

Table 1. Change rates of radiosity

Test ID	Reflection number	Simulation (Shadow of chair)		Test stage (Surface of the table)	
		Average luminosity	Change rate (%)	Average luminosity	Change rate (%)
1	0	11,35	--	78,87	--
2	73	24,56	53,79	121,75	35,22
3	875	56,85	56,80	168,83	27,89
4	1797	61,02	6,83	186,05	9,26
5	2801	62,81	2,85	190,72	2,45
6	3132	64,43	2,52	193,96	1,67
7	3145	64,54	0,17	194,11	0,07
8	3174	64,88	0,52	194,26	0,07

The graphical representation of the average glow and change rates of the shadow belonging to the chair that was generated in the simulation environment in Table 1 are displayed in Figures 13 and 14.

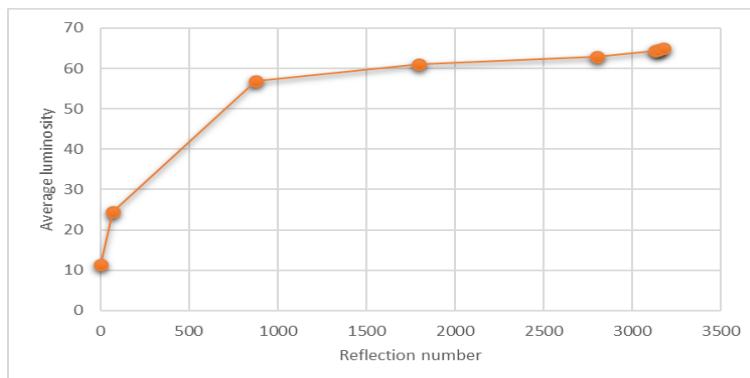


Figure 13. Average brightness change of the shadow of the table according to different numbers of reflection

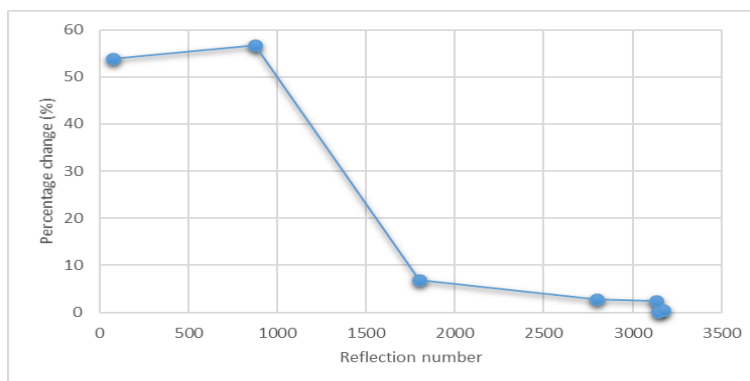


Figure 14. Percentage change in the shadow of the table according to different numbers of reflection

As displayed in Figure 13 and Figure 14, the change in the shadow of the chair after the 3132nd iteration falls below 1%.

The graphical representation of the average glow and change rates on the surface of the table generated in the testing phase in Table 1 is displayed in Figures 15 and 16.

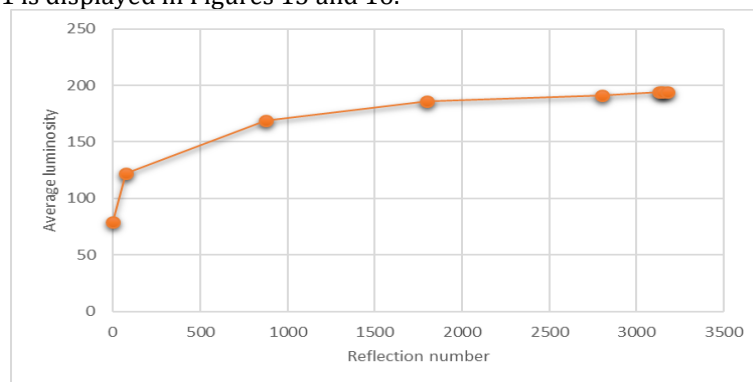


Figure 15. Average brightness change of the shadow of the chair according to different numbers of reflection

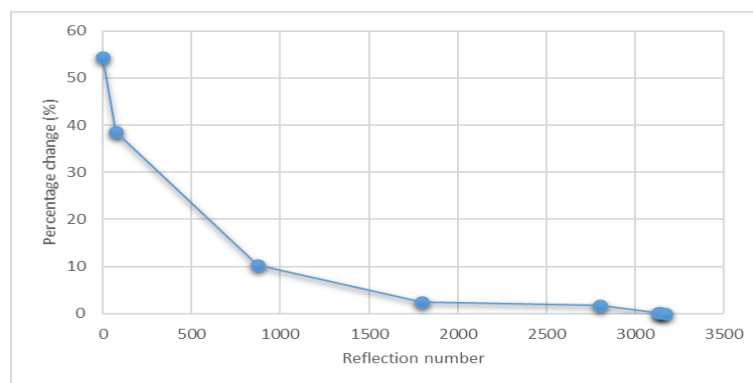


Figure 16. Percentage change in the shadow of the chair according to different numbers of reflection

As displayed in Figure 15 and Figure 16, the average glow changes on the surface of the table used for testing fall below 1% after the iteration no 3132 as in the shadow of the chair.

5. Conclusion

In this study, luminous intensity data of a luminaire was obtained using a computer-operated goniophotometer. These data were transferred to computer environments with radiosity method in a realistic three-dimensional form, and virtual areas based on real data were created. In the virtual environment, the convergence to reality was checked and the termination process was performed through the histogram method with the software.

The system that was developed was primarily offered to the use of engineers and architects engaged in lighting design. With the realistic imaging system that was developed, animations could be developed, accuracy of the images could be questioned according to the direction of the light, and the visual effects of original lighting luminaire in original architectural designs could easily be observed in the computer environment. In addition, the variables of lighting projects were tested through simulations generated in computer environment. The results of the study introduced a photometric realistic infrastructure to the subjects of computer engineering such as computer vision and image synthesis. A photometry based realistic approach was introduced to the computer vision in terms of the relationship between the light sources and colour or the relationship between light and colour. The reflections of objects in the architectural area within each other were obtained with the radiosity method by using the real luminous intensity curves data of the luminaires used in the environments. Therefore, elements such as dark field, shadows and aesthetics have been brought closer to the real model.

While our work is successful, its performance needs to be improved due to its high computational density and memory requirement. Hardware and algorithmic improvement in the system, which provides parallel computational power for calculations, will provide performance improvement.

The level of stopping the radiosity method was decided according to the average brightness measured by the histogram method. When the change in histogram value was close to constant (down to 1%), iteration was stopped by the software. As a result of the tests, it was observed that the change in the brightness value in the histogram decreased below 1% after approximately 3000 iterations.

Teşekkür (Acknowledgement)

Project No. 698-4 entitled "Design and Development of Angular Radiation Meter for Lighting Luminaires" was supported by KOSGEB in 2014.

Çıkar Çatışması (Conflict of Interest)

Yazarlar tarafından herhangi bir çıkar çatışması beyan edilmemiştir. No conflict of interest was declared by the authors.

Kaynaklar (References)

- Baum, D.R., Rushmeier H.E., Winget, J. M., 1989. Improving Radiosity Solutions through the Use of Analytically Determined Form-factors, SIGGRAPH Computer Graphics, 23(3), 325-334.
- Chen, H., Wu, E.H. 1990. An efficient radiosity solution for bump texture generation. SIGGRAPH Computer Graphics, 24(4), 125-134.
- Cohen, M.F., Greenberg, D.P., Immel, D.S., Brock, P.J., 1986. An Efficient Radiosity Approach for Realistic Image Synthesis, IEEE Computer Graphics and Applications, 6(3), 26-35.
- Cohen, M.F., Chen, S.E., Wallace, J.R., Greenberg D.P., 1988. A Progressive Refinement Approach to Fast Radiosity Image Generation. Proceedings of the 15th Annual Conference on Computer Graphics and Interactive Techniques.
- Cohen, M.F., Wallace, J.R., 2012. Radiosity and Realistic Image Synthesis. Elsevier.
- Drucker, S. M., Schröder, P. 1992. Fast radiosity using a data parallel architecture. Third Eurographics Workshop on Rendering
- Goral, C.M., Torrance, K.E., Greenberg, D.P., Battaile, B., 1984. Modeling the Interaction of Light Between Diffuse Surfaces, SIGGRAPH Computer Graphics, 18(3), 213-222.
- Hanrahan, P., Salzman, D., Aupperle, L., 1991. A Rapid Hierarchical Radiosity Algorithm. Proceedings of the 18th Annual Conference on Computer Graphics and Interactive Techniques, 197-206.
- Howell, J.R., Menguc, M.P., Siegel, R., 2010. Thermal Radiation Heat Transfer. CRC press.
- Immel, D.S., Cohen, M.F., Greenberg, D.P., 1986. A Radiosity Method for non-diffuse Environments. SIGGRAPH Computer Graphics, 20 (4), 133-142.
- Nishita, T., Nakamae, E., 1985. Continuous Tone Representation of Three-dimensional Objects Taking Account of Shadows and Interreflection, SIGGRAPH Computer Graphics 19(3), 23-30.
- Purgathofer, W., Zeiller, M. 1992) Fast radiosity by parallelization. Computer Graphics, 171-181.
- Sillion, F. X., Peuch, C., 1994. Radiosity & Global Illumination.
- Sirel, Ş., 1997. Aydınlatma Sözlüğü. YEM Yayınları.
- Sparrow, E.M., 2018. Radiation Heat Transfer, Routledge.
- Wallace, J.R., Cohen M.F., Greenberg, D.P., 1987. A Two-pass Solution to the Rendering Equation: A Synthesis of Ray Tracing and Radiosity Methods, SIGGRAPH Computer Graphics, 21(4), 311-320.
- Wallace, J.R., Elmquist, K.A., Haines, E.A., 1989. A Ray Tracing Algorithm for Progressive Radiosity. Proceedings of the 16th Annual Conference on Computer Graphics and Interactive Techniques.
- Whitted, T., 1979. An improved illumination model for shaded display. 6th annual Conference on Computer graphics and interactive techniques.
- Wolfe, R.J., 2000. 3D Graphics: A Visual Approach. Oxford University Press, Inc.
- Zhu, Y., Peng, Q., Liang, Y., 1988. Peris: A Programming Environment for Realistic Image Synthesis. Computers & Graphics, 12(3-4), 299-307.